Inhibition of $\alpha\beta$ Epithelial Sodium Channels by External Protons Indicates That the Second Hydrophobic Domain Contains Structural Elements for Closing the Pore

Ping Zhang, Gregor K. Fyfe, Irina I. Grichtchenko, and Cecilia M. Canessa
Department of Cellular and Molecular Physiology, Yale University School of Medicine, New Haven, Connecticut 06520-8026 USA

ABSTRACT We have examined the effect of extracellular protons on the activity of epithelial sodium channels (ENaCs). We found that $\alpha\beta$ channels, but not $\alpha\beta\gamma$ or $\alpha\gamma$ channels, are inhibited by low extracellular pH. External protons induced short and long closed states that markedly decreased the open probability of $\alpha\beta$ channels. External protons did not change the single-channel conductance or amiloride binding. Analysis of the proton-induced changes on the kinetics of single channels indicates that at least two protons sequentially bind to the extracellular domain at sites that are not in the ion pathway. Conformational changes induced by protonation of those sites are transmitted to the second hydrophobic domain (M2) of the subunits to induce closure of the pore. The results suggest that elements located in the carboxy-terminal half of M2 participate in the gating mechanism of ENaCs.

INTRODUCTION

Epithelial sodium channels (ENaCs) are prototypes of the ENaC-Deg family of ion channels. In addition to ENaCs, other members include the following: 1) The degenerins from *Caenorhabditis elegans*, which are channels involved in the transduction of mechanical stimuli in a set of neurons in the nematode (Driscoll and Chalfie, 1991; Huang and Chalfie, 1994). 2) The acid-activated channels, known as ASIC, which are a family of cation channels expressed in brain and in dorsal root ganglia (Waldmann and Lazdunski, 1998). The physiological function of the ASIC channels in the nervous system has not been established yet. It has been proposed that they may function as acid sensors and may participate in nociception. 3) FaNaCh, a peptide-activated sodium channel expressed in the ganglion of *Helix aspersa* (Lingueglia et al., 1995). 4) The two recently cloned genes from *Drosophila* named Ripped Pocket (RPK) and Pickpocket (PPK) (Adams et al., 1998). RPK is expressed in early-stage embryos, and PPK is expressed in sensory dendrites in a subset of peripheral neurons. The functions of RPK and PPK in embryogenesis and in the peripheral nervous system from the adult fly are still unknown.

All of these channels are multimeric proteins formed by homologous subunits. All of the subunits share a common structure characterized by the presence of two hydrophobic domains (M1 and M2), short amino- and carboxy-termini inside the cell, and a large extracellular domain with multiple glycosylation sites and conserved cysteine residues (Canessa et al., 1994; Renard et al., 1994). The second transmembrane domain has been shown to determine amiloride affinity and ion selectivity, suggesting that it forms part of the ion pathway (Waldmann et al., 1995; Kellenberger et al., 1999; Fyfe et al., 1999). The extracellular domain is the largest (~65% of the total amino acids) and least characterized of all the domains. Several observations indicate that the extracellular domain plays an important role in the gating of some of these channels. For instance, protonation of the extracellular domain opens ASIC channels (Waldmann and Lazdunski, 1998). Similarly, binding of the neuropeptide FMRFamide opens FaNaCh (Lingueglia et al., 1995). The extracellular domains of the degenerins provide interactions with proteins in the extracellular matrix to madiate the transduction of mechanical stimuli (García-Añoveros et al., 1995).

Several functions have been tentatively assigned to the extracellular domain of ENaC. For instance, it may participate in the assembly of subunits and in the targeting of channels to the plasma membrane. The extracellular domain may also bind or interact with several extracellular modulators. The phenomenon of self-inhibition is thought to be mediated by binding of Na^+ ions to a site located in the external side of the channel protein (Palmer et al., 1998). It has been proposed that the protease CAP1 (Vallet et al., 1998) stimulates ENaC channels by binding or cleaving the extracellular domain of the subunits (Chraïbi et al., 1998). However, in none of these instances is the site to which the agonists bind known, nor is the mechanism that transmits the information from the extracellular domain to the gate to open or close the pore.

Here we have examined the effect of external protons on ENaCs. We show that $\alpha\beta$ channels are inhibited by extracellular protons, whereas $\alpha\beta\gamma$ and $\alpha\gamma$ channels are insensitive to low external pH. The mechanism involved in the inhibition of $\alpha\beta$ channels is not occlusion of the pore but rather changes in the kinetics of $\alpha\beta$ channels. Analysis of the dwell times of the open and closed states indicates that at least two proton-binding events occur at low pH. We

Received for publication 15 June 1999 and in final form 2 September 1999.
Address reprint requests to Dr. Cecilia M. Canessa, Department of Cellular and Molecular Physiology, Yale University School of Medicine, 333 Cedar Street, New Haven, CT 06520-8026. Tel.: 203-785-5892; Fax: 203-785-4951; E-mail: cecilia.canessa@yale.edu.

0006-3495/99/12/3043/09 $2.00

present the simplest kinetic model that accounts for the observations and discuss how protonation of the extracellular domain of ENaCs alters channel gating.

MATERIALS AND METHODS

Oocyte isolation and cRNA injection

Xenopus laevis oocytes were surgically removed from adult female frogs and prepared as previously described (Fyfe and Canessa, 1998). Stage V-VI oocytes were injected with 1 ng each of either α, β, and γ; α and β; or α and γ cRNA from rat ENaC, or with α and γ-β chimera cRNAs. Construction of γ-β chimeras has been described (Fyfe et al., 1998). Oocytes were incubated at 19°C for 2–6 days in amphibian Ringer's supplemented with 10 μM amiloride.

Simultaneous measurements of intracellular pH (pH_i) and membrane potential

pH- and voltage-sensitive microelectrodes were inserted in oocytes for simultaneous measurements of intracellular pH and membrane potential. The chamber was perfused at a rate of 3 ml/min. pH microelectrodes were made of borosilicate glass capillary tubing (1.16 mm ID × 2.0 mm OD; Warner Ins. Corp.) as previously described (Siebens and Boron, 1987). The pH microelectrodes had slopes of −56 to −59 mV per pH unit and resistances of up to 100 MΩ. Voltage and pH microelectrodes were connected to high-impedance electrometers (model FD223; World Precision Instruments, Sarasota, FL). The bath reference electrode was a calomel electrode (no. 1362079; Fisher Scientific, Pittsburgh, PA). pH_i and V_m data were recorded digitally on an 80486-based PC. The analog-to-digital converter (model ADC-30; Contec Microelectronics, San Jose, CA) sampled the V_m and pH_i data at a rate of 0.4 Hz.

Electrophysiology and data evaluation

Electrophysiological recordings were performed using either two-microelectrode voltage-clamp or patch-clamp techniques. For two-microelectrode recordings, current and voltage electrodes were pulled from borosilicate glass, were filled with 3 M KCl, and had resistances less than 1 MΩ. ENaC currents were calculated as the difference in whole-cell current before and after the addition of 50 μM amiloride to the bathing solution. Currents were recorded with an Oocyte Clamp OC-725B (Warner Instrument Corp., Hamden, CT) and digitized at 0.1 kHz (ITC-16; HEKA, Lamprecht, Germany), and the values were stored on the hard disk of a PC. Membrane potential was held at −60 mV. Current-voltage relations were generated by changing the membrane potential from −180 to 80 mV in 20-mV incremental steps of 200 ms duration. *I-V* curves were fitted to the constant field equation. The composition of the standard bath solution was (in mM) 100 Na gluconate, 4 KCl, 2 $CaCl_2$, 10 HEPES, 10 2-(*N*-morpholino)ethanesulfonic acid (MES) (pH adjusted to 7.4, 6.0, 5.0, or 4.0 with either KOH or HCl).

To calculate the apparent pK_a, oocytes were perfused with solutions of progressively lower pH. Measurements were obtained after stabilization of the current to the new value, usually 20–30 s after the pH was changed. Currents were fitted to the equation

$$I/I_{pH\,7.5} = 1/(1 + \{[H^+]/pK_a\}^N), \quad (1)$$

where $[H^+]$ is the concentration of protons in the bathing solution, pK_a is $[H^+]$ at half-maximum inhibition, and N is the Hill coefficient.

To calculate the amiloride K_i, oocytes were perfused with solutions containing increasing concentrations of amiloride. The data were fitted to the equation

$$I/I_{max} = 1/(1 + A/K_i), \quad (2)$$

where A is the amiloride concentration and K_i is the half-inhibition constant.

Single-channel recordings were made from cell-attached patches, and in some cases from inside-out patches. For patch-clamp recordings, pipette-to-membrane seals with resistances of 9–15 GΩ were formed with pipettes made from borosilicate capillary glass by a two-stage pulling and fire-polishing process. An Axopatch 200B amplifier and Digidata 1200B (Axon Instruments, Foster City, CA) interfaced to a PC were used to acquire data at 5 kHz. The data were filtered at 100 Hz during acquisition, using an eight-pole Bessel filter (Frequency Devices, Haverford, MA) and stored directly on the hard drive of a PC. *I-V* relations were constructed by measuring current passing through channels between 0 and −100 mV, and the single-channel conductance was subsequently estimated by linear regression between −20 and −100 mV. Channel open probability was calculated at −40 mV from several minutes of data, using pClamp6. The compositions of pipette solutions were (in mM) 150 LiCl, 1 $CaCl_2$, 1 $MgCl_2$, 10 Tris-MES buffered to pH 7.4, 6.0, 5.0, and 4.0. The bath solution in all patches was (in mM) 150 KCl, 5 EDTA, 10 HEPES (pH adjusted to 7.4 with KOH). Results are expressed as mean ± SEM.

Lists of open- and closed-current interval durations were generated via a half-amplitude threshold crossing criterion. Only patches containing one channel were used in this analysis. All events, independent of duration, were included in the analysis. For this purpose, single-channel data were digitally filtered (Gaussian) at 200 Hz. Histograms containing between 300 and 700 events were generated from individual patches with pHs of 7.4, 6.0, 5.0, or 4.0 in the pipette solutions. Typically, patches performed with pipette solutions of pH 5.0 and 4.0 lasted between 3 and 5 min, limiting the number of events that could be collected from individual patches. Fitting was done with the Simplex-LSQ method of pClamp6 software.

RESULTS

Effect of external protons on the activity of ENaCs

Acidification of the cytoplasm is known to decrease the activity of endogenous ENaCs in principal cells of the cortical collecting tubule (Palmer and Frindt, 1987), as well as in the *Xenopus* oocyte expression system (Chalfant et al., 1999; Abriel and Horisberger, 1999). The consequences of extracellular acidification have not yet been described. Here we examined the effects of pH_o on the activity of ENaC channels formed by various subunit compositions. Studies were done on whole-cell currents, using the two-microelectrode voltage clamp, and on unitary currents, using cell-attached and inside-out patches. For whole-cell experiments, oocytes expressing ENaCs were sequentially exposed to solutions buffered to pH 7.5 and pH 4.0. ENaC currents were calculated by subtracting the whole-cell currents in the absence and presence of 50 μM amiloride. Fig. 1 shows the effect of pH_o 4.0 on $\alpha\beta\gamma$, $\alpha\beta$, and $\alpha\gamma$ channels. Only $\alpha\beta$ channels were blocked by external protons. The effect was rapid, reversible, and reproducible when repeated several times in the same oocyte. Fig. 2 illustrates a representative experiment that shows the time course of the action of pH_o on the currents of $\alpha\beta$ channels. The block by protons was apparent as soon as the solution reached the oocyte and occurred on the same time scale as the amiloride block.

The apparent pK_a of proton block was calculated by examining the inhibition of whole-cell amiloride-sensitive currents by solutions of progressively lower pH (Fig. 3 *A*).

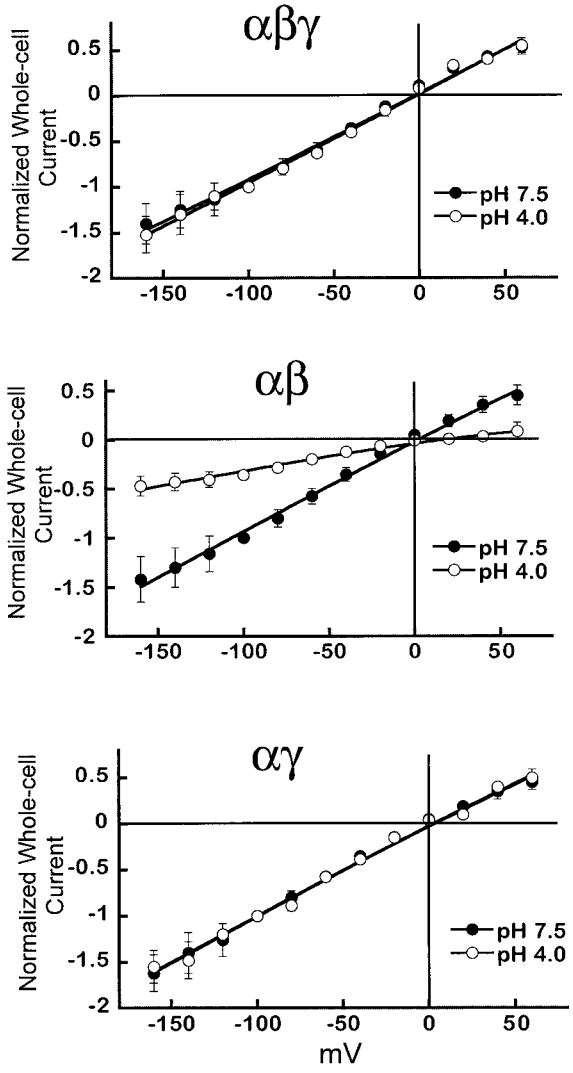

FIGURE 1 Effect of extracellular protons on ENaC channels. Amiloride-sensitive whole-cell currents from oocytes expressing $\alpha\beta\gamma$, $\alpha\beta$, or $\alpha\gamma$ channels were recorded with the two-electrode voltage clamp at various voltages. Values were normalized to the current measured at −100 mV and at pH 7.5. Bathing solutions contained 100 mM Na^+ gluconate, 10 mM HEPES, and 10 mM MES buffered at pH 7.5 (●) or 4.0 (○). Each point represents the mean of six oocytes. Error bars are SEMs. Lines represent the fit of the data, using the constant field equation.

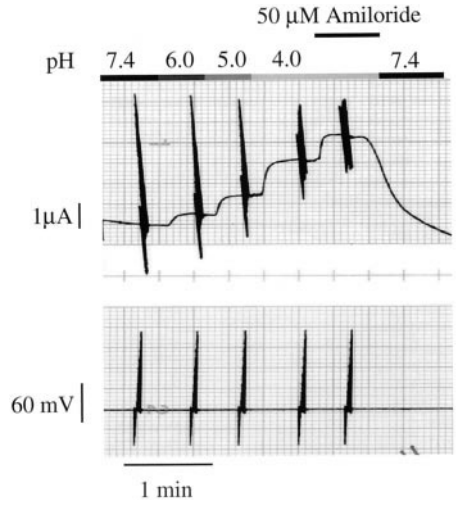

FIGURE 2 Representative experiment of a two-electrode voltage-clamp experiment illustrating the effect of pH_o on the current of an oocyte expressing $\alpha\beta$ channels. The upper panel corresponds to the continuous current recording and the lower panel to the voltage recording. The membrane potential was held at −100 mV; at each different pH the voltage was changed from −180 to 80 mV in 20-mV incremental steps of 200 ms duration. Perfusates were run at a rate of 3 ml/min. The inhibition produced by progressively acidic perfusates occurred as soon as the solutions reached the oocyte. For comparison, the inhibition by amiloride of the current remaining after pH 4.0 is shown.

The calculated apparent pK_a was 4.6, with a Hill coefficient of 1, obtained by fitting the data to Eq. 1 (Fig. 3 *B*).

To be certain that the block was due to external protons and not mediated by acidification of the cytoplasm, we measured intracellular pH with pH-sensitive electrodes. Simultaneous measurements of pH_i and membrane potential were performed in oocytes perfused sequentially with solutions of pH 7.4 and pH 4.0. Perfusion with solutions of pH 4.0 induced small changes in pH_i, of ~0.2 pH units, after 4–7 min. The changes in pH_i took several minutes to develop, in contrast to the almost immediate block of channels revealed by the rapid hyperpolarization of the membrane potential (10–20 mV). A representative experiment is shown in Fig. 4, with pH_i continuous recording in the upper panel and membrane potential in the lower panel.

Protons bind away from the ion pathway

Extracellular protons can block channels by diverse mechanisms, such as occlusion of the pore or altering the gating processes. To determine whether protons bind in the ion pathway of $\alpha\beta$ channels, we investigated 1) voltage dependence of the proton block, 2) effects of protons on amiloride block, and 3) effects of external Na^+ concentration.

Proton block was measured at various voltages, from −160 to −20 mV, and plotted as the fractional inhibition of whole-cell currents produced by pH 4.0 and pH 5.0. Fig. 5 shows that the fraction of current inhibited by low pH was the same at all voltages, indicating that the block is not voltage dependent.

Amiloride inhibits $\alpha\beta$ channels by occluding the entrance of the pore with a K_i of 1 μM measured at pH 7.4 (Fyfe and Canessa, 1998). To investigate possible interactions between amiloride and external protons we measured the amiloride K_i of $\alpha\beta$ channels with solutions of pH 4.0. Fig. 6 shows that the amiloride K_i measured at pH 4.0 was 1 μM. This value is identical to the one obtained with pH 7.4, suggesting that amiloride and protons bind to different sites.

If the mechanism of proton block involves binding in the ion pathway, varying the external concentrations of the permeant ion is expected to affect the degree of proton block. Therefore, we examined the effect of changing the Na^+ concentration of the external solution from 30 to 150

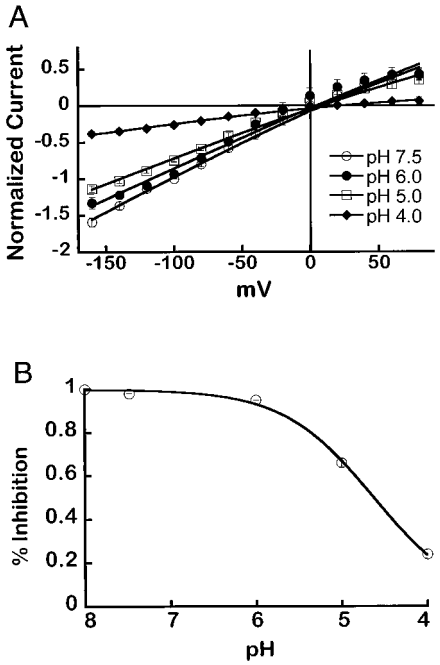

FIGURE 3 Block of $\alpha\beta$ channels by external protons. (*A*) Whole-cell amiloride-sensitive currents of $\alpha\beta$ channels were progressively inhibited by lowering the pH of the bathing solutions from 7.4 to 6.0, 5.0, and 4.0. Currents were normalized to the value measured at pH 7.5 and at −100 mV. Data points were fitted to the constant field equation. (*B*) Currents measured at several pHs and at −100 mV membrane potential were plotted as a function of external pH. Fitting of the data to Eq. 1 gave values for the apparent pK_a and Hill coefficient of 4.6 and 1, respectively. Each point represents data from five to eight oocytes. Error bars are SEM; some are smaller than the data symbols.

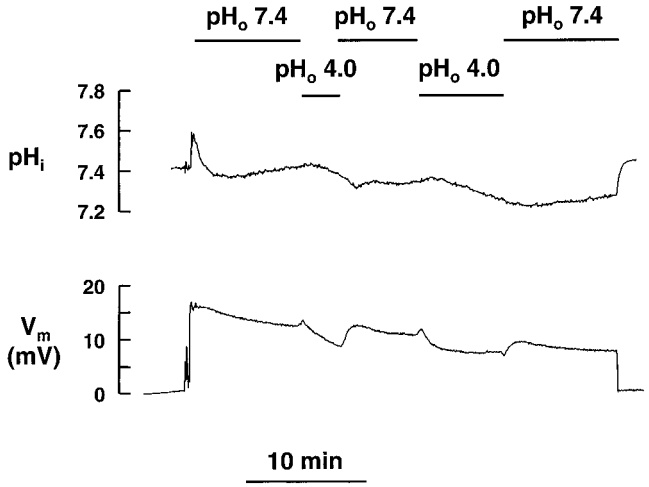

FIGURE 4 Simultaneous measurements of pH_i and V_m from a representative oocyte expressing $\alpha\beta$ channels. The initial pH_i of the oocyte was 7.4. After 3 or 7 min of perfusion with solution at pH 4.0, the pH_i slowly changed by 0.2 pH units. V_m showed a small hyperpolarization with solutions at pH 4.0. With a perfusion rate of 3 ml/min the changes in V_m were rapid and reversible. The bars under pH_o 7.4 and pH_o 4.0 indicate the duration of perfusion with solutions at the corresponding pH.

mM Na^+. Fig. 7 shows amiloride-sensitive Na^+ currents normalized to the current measured at −100 mV in the presence of 30 mM Na^+ or 150 mM Na^+ in the external solution. In 30 mM Na^+, the reversal potential was shifted to the left, and the *I-V* curves had a slight outward rectification. Both findings reflect a high concentration of intracellular Na^+. The inhibition of currents by pH 4.0 was the same regardless of the external Na^+ concentration.

Taken together, these results suggest that the proton-binding site(s) is located outside of the membrane electrical field and away from the channel pore.

Protons block $\alpha\beta$ channels by inducing closed states

To elucidate the mechanism(s) of proton inhibition, we investigated the effect of low pH_o at the single-channel level, using cell-attached and inside-out configurations of the patch-clamp technique. In experiments in which the pH of the pipette solution was 6.0, 5.0, or 4.0, we did not observe changes in the magnitude of the unitary currents. The single-channel conductance was 10 pS at both pH 7.4 and pH 4.0, indicating that protons decrease $\alpha\beta$ channel currents by a mechanism distinct from fast occlusion of the pore.

In contrast, protons markedly changed the kinetics of $\alpha\beta$ channels and induced new closed states. With pH 7.4, the kinetics of $\alpha\beta$ channels were characterized by very long openings (mean open time = 2000 ± 252 ms) and infrequent and brief closures (mean closed time = 8.2 ± 1.5 ms). The open probability was very high; in fact it was close to 1 (P_o = 0.99) (Fig. 8 *A*). Increasing the concentrations of external protons reduced the P_o progressively and changed the kinetics of $\alpha\beta$ channels. With pH 6.0 in the pipette solution, brief (17.7 ± 4.3 ms) and more frequent closures were evident (Fig. 8 *B*); however, the P_o remained high (P_o = 0.97 ± 0.1). With pH 5.0, much longer closures

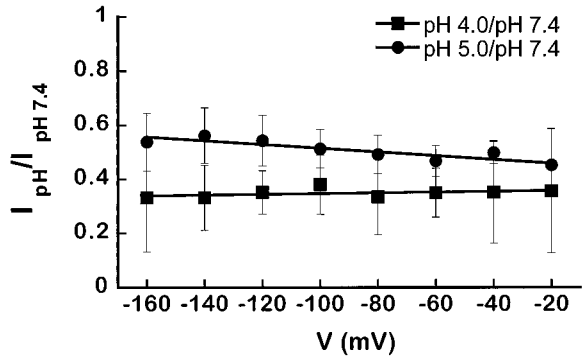

FIGURE 5 Inhibition of $\alpha\beta$ channels by external protons examined at various voltages (−180 to 80 mV). Whole-cell amiloride-sensitive currents of oocytes expressing $\alpha\beta$ channels were measured with solutions buffered at pH 7.4, 5.0, and 4.0. The effect of pH is plotted as the fractional inhibition of current $I_{pH\ 5.0}/I_{pH\ 7.4}$ and $I_{pH\ 4.0}/I_{pH\ 7.4}$ at each voltage. The slopes of the lines connecting the data points indicate that proton block is not voltage dependent. Each point represents data from eight oocytes. Error bars represent SEM.

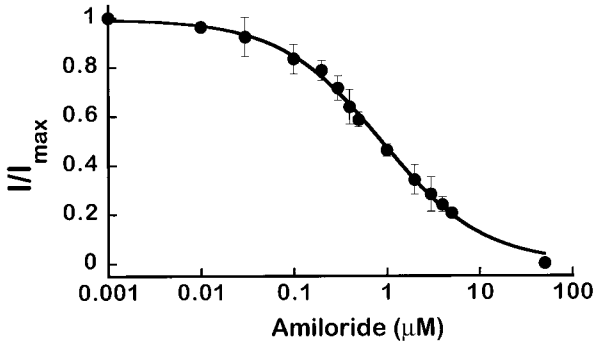

FIGURE 6 Amiloride inhibition of $\alpha\beta$ channels at pH 4.0. The amiloride K_i of $\alpha\beta$ of channels was measured with solutions buffered to pH 4.0. Membrane potential was held at −60 mV. Solutions contained 100 mM Na^+. Amiloride K_i calculated using Eq. 1 was 1 μM, which is identical to the K_i measured at pH 7.4. Data points are the mean ± SEM of six to eight independent measurements from different oocytes.

appeared (370 ± 56 ms) (Fig. 8 *C*), without changes in the frequency of the short closures. The long closures decreased the P_o to 0.5 ± 0.05. At pH 4.0, the mean P_o was reduced to 0.3 ± 0.02, mainly because of more frequent long closures (Fig. 8 *D*).

To confirm that the changes in P_o were induced by external protons and not by acidification of the cytoplasm, we performed experiments using inside-out patches, in

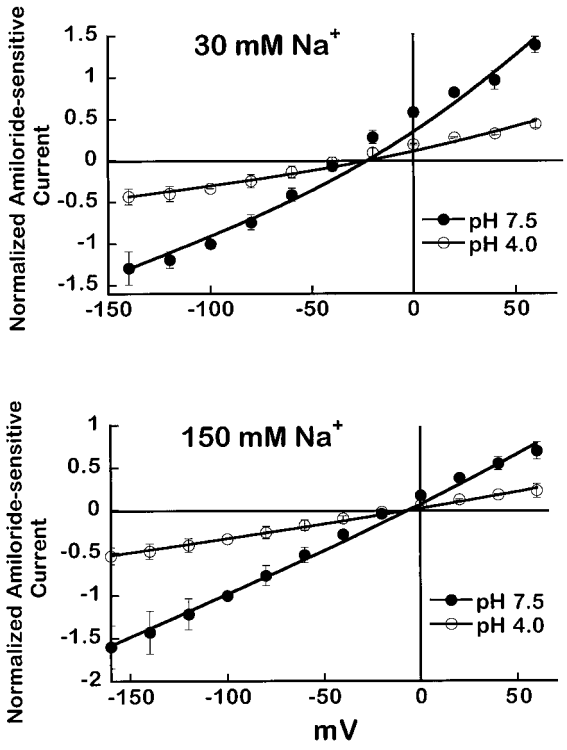

FIGURE 7 Proton block of $\alpha\beta$ channels examined with solutions containing 30 mM and 150 mM Na^+ gluconate. The fractional inhibition of amiloride-sensitive whole-cell currents by pH 4.0 was similar in solutions containing 30 or 150 mM Na^+. Each point represents the mean ± SEM of five oocytes.

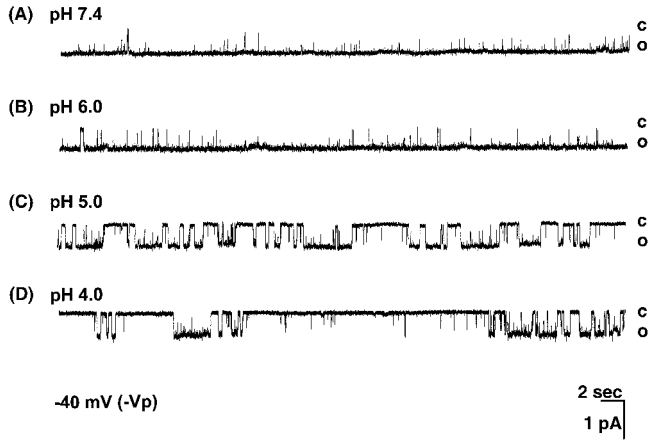

FIGURE 8 Representative examples of unitary currents of $\alpha\beta$ channels recorded in cell-attached patches containing 150 mM LiCl in the pipette solution buffered to pH 7.4 (*A*), 6.0 (*B*), 5.0 (*C*), and 4.0 (*D*). $-V_p$ (the negative value of the pipette holding potential) was −40 mV. The current amplitude and the time scale are indicated on the scale bars.

which the pH of the pipette solution was kept at 4.0 and the pH of the bath solution was 7.4 (Fig. 9). The results were indistinguishable from the ones obtained with cell-attached patches. These experiments further demonstrate that protons bind to the extracellular side of the channels.

The decrease in P_o observed at the single-channel level completely accounted for the pH inhibition in the whole-cell experiments, indicating that the effect of protons was exclusively mediated by changes in channel kinetics.

More than one proton binds to the channel

To better understand the mechanism by which external protons change the P_o of $\alpha\beta$ channels, we examined the kinetics of inhibition by low pH_o in more detail. Dwell-time histograms were constructed from the open and closed

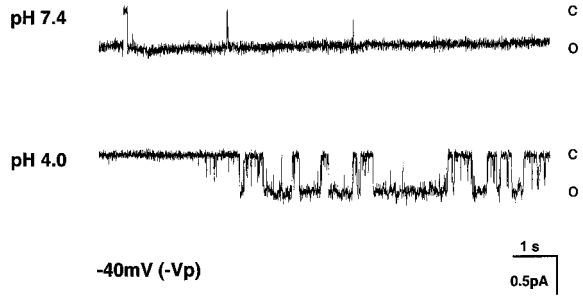

FIGURE 9 Representative experiments of inside-out patches performed with pipette and bath solutions of pH 7.4 (*top*) and pipette solution of pH 4.0 and bath solution of 7.4 (*bottom*). Both records show single channels. The closed and open states are indicated by C and O, respectively. The amplitude of the unitary currents is the same at pH 7.4 and pH 4.0. However, with solutions of pH 4.0 in the pipette, the channel exhibits long and short closures. $-V_p$ (the negative value of the pipette holding potential) was −40 mV. The current amplitude and the time scale are indicated on the scale bars.

events with pH 7.4, 6.0, 5.0, and 4.0. High filtering was necessary to obtain clean records because of the low magnitude of the unitary currents (~0.5 pA at −40 mV) and because recordings with pipette solutions of low pH had a tendency to be noisy. Although the data used to generate the histograms shown in Fig. 10 were filtered at 100 Hz, no significant differences were detected when they were filtered at 1 kHz, indicating that we did not miss many short events. In general, patches with pipette solutions of pH 5.0, and in particular of pH 4.0, were stable for ~5 min; longer recordings were difficult to maintain. The inability to perform long recordings at low pHs hampered the detection of very long closed events. This is reflected in the closed-state histograms, where the number and duration of the observed events were reduced from the actual values.

At pH 7.4, channels exhibited a single long open state of 2000 ms duration and a single short closed state of 8.2 ms duration, as indicated by the histograms fitted well with only one exponential. At pH 6.0, the histogram of the closed states showed more frequent closed events, which reduced the mean length of the open state to 630 ms. The short closures had a mean duration of 17 ms, and both histograms were well fitted to single exponentials. With pH 5.0 and 4.0 the histograms of the open and closed states were best fitted with two exponentials, indicating the existence of two distinct openings, a short and a long one, and of two distinct closures, a short and a long one.

The appearance of a new closed state produced by increased proton concentration could be explained by postulating sequential binding of protons (at least two) to the channel. A simple model that accounts for the observations is presented in Fig. 11. At pH 7.4 the channel does not bind protons and has a very stable open state (O_0) that is infrequently interrupted by short closures (C_{S0}). At pH 6.0, protons bind to the channel (O_1) and induce more frequent short closures (C_{S1}), the duration of which was similar to the one at pH 7.4. The site occupied at low proton concentration seems to saturate at pH 6.0 because further decreases in pH did not increase the frequency of these events. At lower pH, more protons bind to the channel such that the open state (O_2) can adopt either a short closure (C_{S2}) or a long closure (C_L). As can be seen from records at pH 5.0

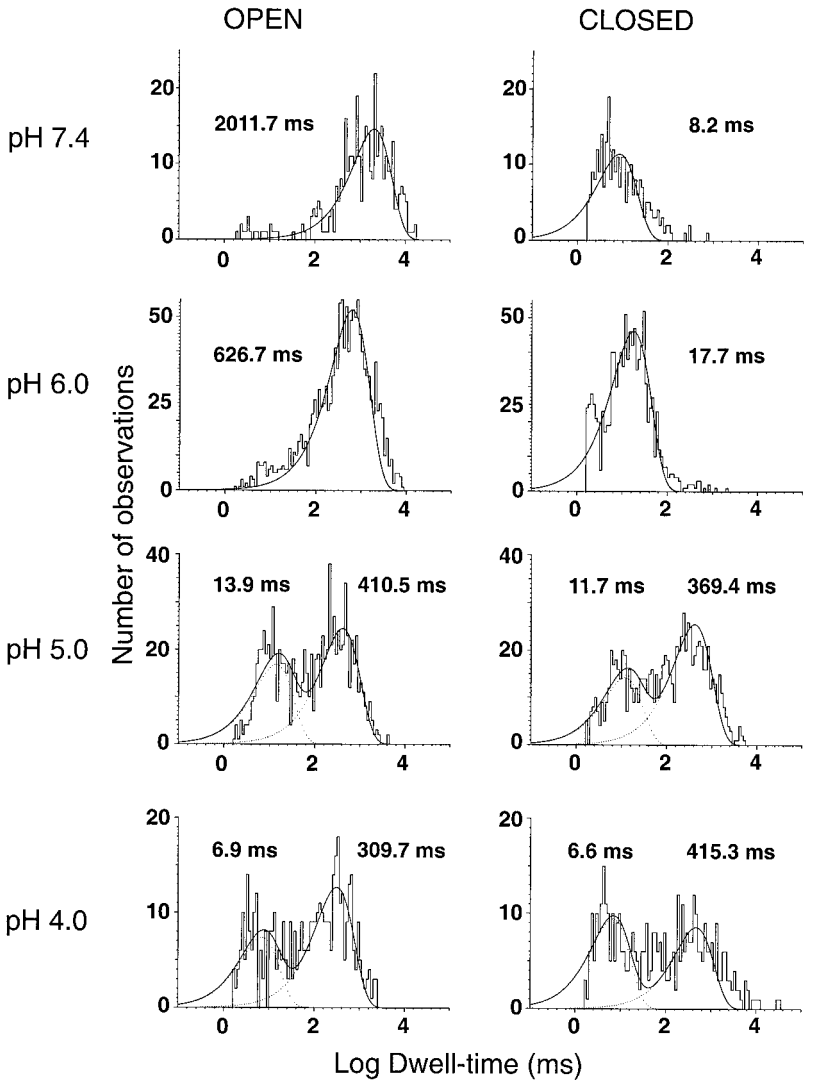

FIGURE 10 Dwell-time histograms of open and closed events recorded from single $\alpha\beta$ channels in the presence of pipette solutions buffered at pH 7.4, 6.0, 5.0, and 4.0. The solid lines at pH 7.4 and pH 6.0 are fits of the data to a single exponential. The solid lines at pH 5.0 and pH 4.0 are fits to a sum of two exponential functions with short and long time constants. The time constants (ms) from each exponential are shown for the open and closed states. Histograms were constructed with data collected from seven to nine patches containing single channels.

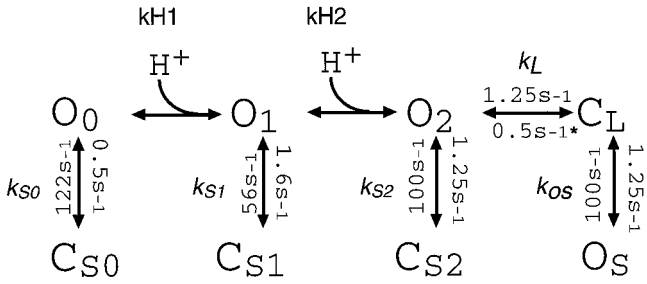

FIGURE 11 Kinetic model for proton block of $\alpha\beta$ channels. The open and closed states are indicated by O and C. O_0, O_1, and O_2 represent the open states without protons, with one or two protons bound, respectively. The open states without or with one or two protons can adopt short closed states, represented by C_{S0}, C_{S1}, and C_{S2}, respectively. The O_2 state can also enter a long closed state (C_L). From the C_L state, channels can open to O_2 or to a short (O_S) open state. The values for the rate constants for each of the transitions to the open and closed states are shown. See the Discussion for a full explanation.

and 4.0 (Fig. 8, *C* and *D*), the long closures are interrupted by short openings (O_S); therefore, the C_L state can open either to the long (O_2) or short open (O_S) state.

When 1 μM amiloride was present in pipette solutions of pH 4.0, we observed long closures induced by protons and, in addition, brief and frequent transitions interrupting the long open state (Fig. 12). The mean blocked time induced by amiloride (30 ms at -40 mV) was voltage dependent, as previously shown (Fyfe and Canessa, 1998), whereas the proton-induced closures were voltage independent.

Where do protons interact with the channel?

The finding that $\alpha\beta$ but not $\alpha\gamma$ channels are blocked by lowering the external pH suggested that protons may bind to the β subunit. To test this hypothesis, we expressed channels formed by wild-type α subunits and chimeras constructed between β and γ subunits. The γ-β chimeras contained the amino-terminus of γ and carboxy-terminus of β. Four γ-β chimeras, having the junction between γ and β progressively displaced toward the carboxy-terminus of β, were examined. A schematic representation of the γ-β chimeras tested is shown in Fig. 13. A pH_o of 4.0 blocked 70–80% of the currents from the first three chimeras. Only the last chimera, which contains most sequences from γ and only the carboxy-terminal segment of the second transmembrane domain from β, was insensitive to external protons. These results indicate that elements located in M2 are required to confer pH sensitivity. Because the previous experiments showed that protons do not bind in the ion pathway, the protonation sites must be located in the extracellular domain.

The results argue that, even though protons bind to the extracellular domain, the sensitivity to external protons depends on the second transmembrane domain of the subunits.

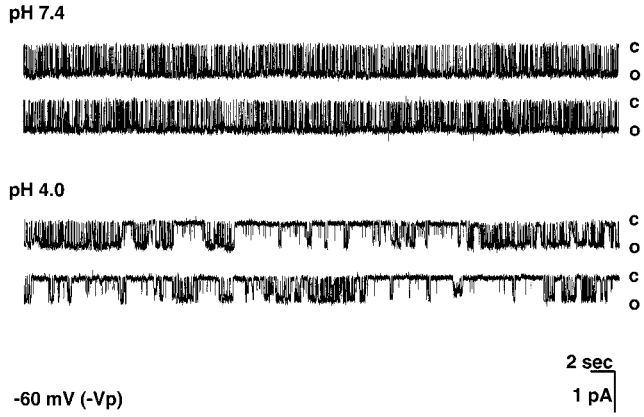

FIGURE 12 Recording of unitary currents of $\alpha\beta$ channels with 1 μM amiloride in the pipette. The pipette solution was buffered at pH 7.4 (*A*) and pH 4.0 (*B*). The trace at pH 7.4 shows long openings interrupted by the flickering block of amiloride. The P_o of the channel is ~0.6. The trace at pH 4.0 shows closures induced by protons, and the openings are interrupted by amiloride block. $-V_p$ (the negative value of the pipette holding potential) was -60 mV. The current amplitude and the time scale are indicated on the scale bars.

DISCUSSION

In this work we have shown that external protons decrease the activity of $\alpha\beta$ channels by altering the kinetics and reducing the P_o. We conclusively ruled out the possibility that protons could be blocking channels from the cytoplasmic side. First, in experiments that examined whole-cell currents where oocytes were perfused with solutions of low pH, we observed very rapid changes in channel currents upon exposure to solutions of different pHs. Currents were blocked in a few seconds, the time required for the solution to reach the perfusion chamber. Similarly, the block was relieved very rapidly by returning to a solution of pH 7.4. If the block were mediated by lowering pH_i, the changes in current would have taken longer because of the low proton

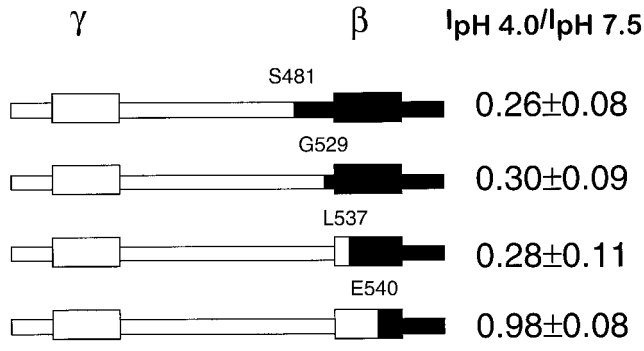

FIGURE 13 Schematic representation of γ-β chimeras and fractional inhibition of amiloride-sensitive currents by external pH. In white and black are sequences corresponding to γ and β subunits, respectively. The transmembrane domains are indicated by boxes. The letters and numbers above each chimera indicate the first residue corresponding to the β subunit. Sensitivity to external protons was expressed as the ratio of currents at pH 4.0 over those at pH 7.5. The first three chimeras were inhibited by low pH_o, whereas the γ-βE540 chimera was insensitive to low pH_o.

permeability of the plasma membrane and the large cytosolic buffering capacity of the oocytes. In addition, if protons readily permeate the plasma membrane, we should have seen inhibition of $\alpha\beta\gamma$ and $\alpha\gamma$ channels, which are also known to be sensitive to intracellular acidification (Palmer and Frindt, 1987; Chalfant et al., 1999; Abriel and Horisberger, 1999). When the cytosolic pH was measured with a pH-sensitive electrode inserted into the oocyte, we detected pH_i changes of ~0.2 units of pH after 7 min of perfusion with solutions of pH 4.0. The small changes in pH_i also suggest that $\alpha\beta$ channels are not permeable to protons.

Changes in intracellular pH were not a concern in experiments using cell-attached patches, because the whole cell was exposed to pH 7.4 and only the small area of the patch pipette was exposed to low pH. In these experiments, as well as in those with inside-out patches with a pipette solution of pH 4.0 and a bath solution of pH 7.4, pH_o had the same effect. Therefore, inhibition of $\alpha\beta$ channels is mediated by external and not internal protons.

The next question was whether protons block $\alpha\beta$ channels by binding to the ion pore or by other mechanisms. First, we showed that protons did not change the single-channel conductance, indicating that the block does not involve screening of surface charges or titration of negatively charged residues at the entrance of the pore. In addition, we demonstrated that proton block was voltage independent, was not affected by changes in the concentration of external Na^+, and did not alter the kinetics of amiloride block. Together, these results indicate that protons do not occlude the ion pore. In contrast, low pH_o changed the kinetics of $\alpha\beta$ channels mainly by generating new closed states that markedly reduced the P_o. Analysis of the histograms of the dwell times of open and closed states revealed two open and two closed states induced by low pH_o, suggesting sequential binding of at least two protons, as depicted in the model of Fig. 10. The rate constants for each of the transitions were calculated from the mean dwell times obtained by fitting the probability density functions. The model was used to predict the P_o at various external pHs according to the following expressions:

$$[O_1] = [H]^*k_{H1}^*[O_0]$$

$$[O_2] = [H]^*k_{H2}^*[O_1] \Rightarrow [O_2] = [H]^{2*}k_{H1}^*k_{H2}^*[O_0]$$

$$[O_2] = k_L^*[C_L] \Rightarrow [C_L] = [H]^{2*}k_{H1}^*k_{H2}^*[O_0]/k_L$$

$$[O_2] = k_{S2}^*[C_{S2}] \Rightarrow [C_{S2}] = [H]^{2*}k_{H1}^*k_{H2}^*[O_0]/k_{S2}$$

$$[O_0] = k_{S0}^*[C_{S0}] \Rightarrow [C_{S0}] = [O_0]/k_{S0}$$

$$[O_1] = k_{S1}^*[C_{S1}] \Rightarrow [C_{S1}] = [H]^*k_{H1}^*[O_0]/k_{S1}$$

$$[O_S] = [C_L]/k_{OS} \Rightarrow [O_S] = [H]^{2*}k_{H1}^*k_{H2}^*[O_0]/k_L^*k_{OS}$$

$$[O_0] + [O_1] + [O_2] + [O_S] + [C_{S0}] + [C_{S1}] + [C_{S2}] + [C_L] = 1$$

$$[O_0]^*\{1 + 1/k_{S0} + [H]^*k_{H1}^*(1 + 1/k_{S1}) + [H]^{2*}k_{H1}^*k_{H2}^*(1 + 1/k_{S2} + 1/k_L + 1/k_L^*k_{OS})\} = 1$$

$$P_o = [O_0] + [O_1] + [O_2] + [O_S]$$

$$P_o = \frac{1 + [H]k_{H1} + [H]^{2*}k_{H1}^*k_{H2} + ([H]^{2*}k_{H1}^*k_{H2}/k_L^*k_{OS}^*)}{1 + 1/k_{S1} + [H]^*{}_{H1}^*(1 + 1/k_{S1}) + [H]^{2*}k_{H1}^*k_{H2}^*(1 + 1/k_{S2} + 1/k_L + 1/k_L^*k_{OS})}$$

$$k_{H1} = 10^6\ M^{-1} \quad k_{S0} = 244 \quad k_L = 0.4^*$$
$$k_{H2} = 10^5\ M^{-1} \quad k_{S1} = 334 \quad k_{OS} = 80$$
$$k_{S2} = 80$$

k_{H1} was assigned a value of $10^6\ M^{-1}$ because the first protonation seemed to saturate at pH 6.0; no significant increase in the frequency of short closures was observed at lower pH. The rate constant $k_L = 0.4^*$ was obtained by using a dwell time of 2000 ms for the long closed states (C_L) instead of 400 ms. We know that 400 ms is an underestimate of the duration of C_L. In many instances, we observed very long closures (>1000 ms). However, the long closures were underrepresented in the histograms because patches at pH 4.0 could not be maintained for more than 5 min. Because long closures used most of the recording time, fewer long events were collected.

Solving the above P_o equation for pH 7.4, 5.0, and 4.0, we obtained values of 0.99, 0.45, and 0.31, respectively. The same calculations using 1000 ms for C_L gave a P_o for pH 7.4, 5.0, and 4.0 of 0.99, 0.62, and 0.46, respectively. These values are very close to the actual data, indicating that the proposed model accounts for the observations.

The finding that $\alpha\beta$ but not $\alpha\gamma$ channels were blocked by protons suggested that subunit composition determines the sensitivity to pH_o. An interpretation could have been that protons bind to the β subunit. However, when this possibility was investigated by expressing γ-β chimeras, we could replace all of the extracellular domain from γ sequences and still observe proton block. The crucial region that conferred proton sensitivity on the chimeras was located in the second transmembrane domain, specifically in the carboxy-terminal half of M2. This region would be located beyond the narrowest point of the channel pore, which has been proposed to be at the level of residue S531 in the β subunit (Kellenberger et al., 1999).

The results from this work indicate that at least two protons bind to the extracellular domain of any of the subunits of ENaC away from the ion pore. However, proton binding is not enough to close the channels. The sensitivity to low pH_o depends on the second transmembrane domains, where we propose some of the gating mechanisms are located. Protonation of residues in the extracellular domain produces conformational changes that are transmitted to the M2 region to induce closures of the pore. While the initial segment of the second transmembrane domain determines amiloride affinity and ion selectivity, the distal region,

closer to the cytoplasmic side, may be involved in gating the pore.

Our results have features in common with the recently crystallized K^+ channel from *Streptomyces lividans* (SKC1) (Doyle et al., 1998) that also exhibits pH-dependent gating (Cuello et al., 1998). The subunits of ENaC and SKC1 have only two transmembrane domains, and M2 forms the ion pathway in both channels. In contrast to ENaC, SKC1 has very few residues facing the extracellular side; most are located in the cytosolic side. Under basal conditions, SKC1 is closed, but it opens upon acidification (pH 3.5) of the cytoplasmic side. Perozo et al. (1998) measured a large conformational change in the carboxy-terminal end of M2 after lowering the pH, suggesting that the gate of SKC1 is located in the terminal end of M2. The data from our work support a similar gating mechanism for ENaC channels.

In addition, this work has implications that extend to other members of the ENaC-Deg family of ion channels, such as ASIC. In basal conditions ASIC channels are closed, but they open upon exposure to low pH_o. The mechanism of proton activation of ASIC channels has not been worked out yet, but many features seem to be common with ENaC.

Although regulation of ENaCs by pH_o is not relevant under normal physiological conditions, they may be important in pathological conditions such as pseudohypoaldosteronism type 1 (PHA1), where lack of expression of the γ subunit generates $\alpha\beta$ channels. In the cortical collecting tubule of the kidney, ENaCs are exposed to pH_o as low as 5.0. It is conceivable that the waste of salt by the kidneys of patients with PHA1 is worsened by proton block of $\alpha\beta$ channels.

We thank Dr. Fred Sigworth for his suggestions.

This work was done during the tenure of an American Heart Association Postdoctoral Fellowship (GKF) and was supported by National Institutes of Health grant HL56163.

REFERENCES

Abriel, H., and J.-D. Horisberger. 1999. Feedback inhibition of rat amiloride-sensitive epithelial sodium channels expressed in *Xenopus laevis* oocytes. *J. Physiol. (Lond.).* 516:31–43.

Adams, C. M., M. G. Anderson, D. G. Motto, M. P. Price, W. A. Anderson, and M. J. Welsh. 1998. Ripped pocket and pickpocket, novel *Drosophila* DEG/ENaC subunits expressed in early development and in mechanosensory neurons. *J. Cell. Biol.* 140:143–152.

Canessa, C. M., A.-M. Merillat, and B. C. Rossier. 1994. Membrane topology of the epithelial sodium channel α-subunit: identification of N-linked glycosylation sites and of start and stop transfer signals used in intact cells. *Am. J. Physiol.* 267:C1682–C1690.

Chalfant, M. L., J. S. Denton, K. Bakhram, K. Berdiev, I. I. Ismailov, D. J. Benos, and B. A. Stanton. 1999. Intracellular H^+ regulates the α-subunit of ENaC, the epithelial Na^+ channel. *Am. J. Physiol.* 276:C477–C486.

Chraïbi, A., V. Vallet, D. Firsov, S. Kharoubi Hess, and J.-D. Horisberger. 1998. Protease modulation of the activity of the epithelial sodium channel expressed in *Xenopus* oocytes. *J. Gen. Physiol.* 111:127–138.

Cuello, L. G., J. G. Romero, D. M. Cortes, and E. Perozo. 1998. pH-dependent gating in the *Streptomyces lividans* K^+ channel. *Biochemistry.* 37:3229–3236.

Doyle, D. A., J. M. Cabral, R. A Pfuetzner, A. Kuo, J. M. Gulbis, S. L. Cohen, B. T. Chait, and R. MacKinnon. 1998. The structure of the potassium channel: molecular basis of K^+ conduction and selectivity. *Science.* 280:69–77.

Driscoll, M., and M. Chalfie. 1991. The mec-4 gene is member of a family of *Caenorhabditis elegans* genes that can mutate to induce neuronal degeneration. *Nature.* 349:588–593.

Fyfe, G. K., and C. M. Canessa. 1998. Subunit composition determines the single channel kinetics of the epithelial sodium channel. *J. Gen. Physiol.* 112:423–432.

García-Añoveros, J., C. Ma, and M. Chalfie. 1995. Regulation of *Caenorhabditis elegans* degenerin proteins by a putative extracellular domain. *Curr. Biol.* 5:441–448.

Huang, M., and M. Chalfie. 1994. Gene interactions affecting mechanosensory transduction in *Caenorhabditis elegans. Nature.* 367:467–470.

Kellenberger, S., I. Gautschi, and L. Schild. 1999. A single point mutation in the pore region of the epithelial Na^+ channel changes ion selectivity by modifying molecular sieving. *Proc. Natl. Acad. Sci. USA.* 96: 4170–4175.

Lingueglia, E. L., G. Champigny, M. Lazdunski, and P. Barbry. 1995. Cloning of the amiloride-sensitive FMRFamide peptide-gated sodium channel. *Nature.* 378:730–733.

Palmer, L. G., and G. Frindt. 1987. Effects of cell Ca and pH on Na channels from rat cortical collecting tubule. *Am. J. Physiol.* 253: F333–F339.

Perozo, E., D. M. Cortes, and L. G. Cuello. 1998. Three-dimensional architecture and gating mechanism of a K^+ channel studied by EPR spectroscopy. *Nature Struct. Biol.* 5:459–469.

Renard, S., E. Lingueglia, N. Voilley, M. Lazdunski, and P. Barbry. 1994. Biochemical analysis of the membrane topology of the amiloride-sensitive Na^+ channel. *J. Biol. Chem.* 269:12981–12986.

Siebens, A. W., and W. F. Boron. 1987. Effect of electroneutral luminal and basolateral lactate transport on intracellular pH in salamander proximal tubules. *J. Gen. Physiol.* 90:799–831.

Vallet, V., A. Chraibi, H-P. Gaeggeler, J.-D. Horisberger, and B. C. Rossier. 1998. An epithelial serine protease activates the amiloride-sensitive sodium channel. *Nature.* 389:607–610.

Waldmann, R., G. Champigny, and M. Lazdunski. 1995. Functional degenerin-containing chimeras identify residues essential for amiloride-sensitive Na^+ channel function. *J. Biol. Chem.* 270:11735–11737.

Waldmann, R., and M. Lazdunski. 1998. H^+-gated cation channels: neuronal acid sensors in the NaC/DEG family of ion channels. *Curr. Opin. Neurobiol.* 8:418–424.